Combining multiphoton excitation microscopy with fast microiontophoresis to investigate neuronal signaling

Espen Hartveit and Margaret Lin Veruki

University of Bergen, Department of Biomedicine, Bergen, Norway

Corresponding author: Espen Hartveit, University of Bergen, Department of Biomedicine, Jonas Lies vei 91, N-5009 Bergen, Norway.

Email address: espen.hartveit@biomed.uib.no

Number of figures: 7

Number of tables: 1

Running head: MPE microscopy-guided microiontophoresis

i. Abstract

Multiphoton excitation (MPE) microscopy allows subcellular structural and functional imaging of neurons and can be combined with techniques for activating postsynaptic receptors at spatial and temporal scales that mimic normal synaptic transmission. Here, we describe procedures for combining MPE imaging of dye-filled neurons with fast microiontophoresis, by which neurotransmitter agonists can be applied from high-resistance micropipettes with subcellular resolution. With adequate compensation of the pipette capacitance, the effective time constant of the pipette is reduced and this permits application of very brief pulses of receptor agonist (≤1 ms). The consequent high temporal and spatial resolution leads to the high specificity required for single-synapse investigations. The chapter includes detailed procedures for electrophysiological whole-cell recording, structural and functional (Ca^{2+}) MPE imaging of dye-filled neurons, targeting a microiontophoresis pipette to a specific subcellular compartment of a dye-filled neuron under visual control, and capacitance compensation of the microiontophoresis pipette, as well as examples of experimental results that can be obtained.

ii. Keywords

Microiontophoresis, Ion channels, Ionotropic receptors, Receptor localization, Multiphoton excitation microscopy, Patch-clamp electrophysiology

1 Introduction

In conventional chemical synapses of the central nervous system, the organization and specialization of the pre- and postsynaptic structures convey high precision in both the spatial and temporal domains (for review, see [1]). When neurotransmitter molecules are released from presynaptic vesicles, they diffuse across the narrow synaptic cleft and bind to and activate heterogeneous populations of receptors, located in the membranes of postsynaptic neurons. The different types of receptors typically differ in functional properties such as affinity for the neurotransmitter, single-channel

conductance, kinetics, selectivity and permeability for specific ions, developmental regulation, and influence on downstream signaling pathways [2, 3]. Ideally, the investigator would like to study and manipulate functional properties at both pre- and postsynaptic sites with subcellular (single-synapse) resolution in intact, functioning neural tissue. This includes mechanisms of presynaptic exocytosis, properties of pre- and postsynaptic receptors, and postsynaptic signaling and transduction mechanisms. The advent of 2-photon (2P) or multiphoton excitation (MPE) microscopy has enabled investigations at the required level of spatial and temporal resolution [4], with respect to both structural imaging of subcellular neuronal components and functional imaging of pre- and postsynaptic intracellular Ca^{2+} signals within intact neural tissue [5]. As such, MPE microscopy does not enable activation of postsynaptic receptors, but when combined with either 2P/MP uncaging of neurotransmitter [5] (see chapters by Tran-Van-Minh et al. and Stein et al., this volume) or fast microiontophoresis [6], such receptors can be activated at spatial and temporal scales that (approximately) mimic and are directly relevant for normal chemical synaptic transmission. Here, we describe the combination of MPE microscopy (for structural and functional imaging) and fast microiontophoresis.

Ca^{2+} plays important roles as a second messenger in a large number of intracellular signaling pathways [7] and changes in intracellular Ca^{2+} concentration can be triggered by a number of different mechanisms acting through receptors and ion channels located in the plasma membrane and intracellular organelles of neurons and other cells. Over the last 20 years, powerful imaging methods have been developed that allow the measurement of Ca^{2+} signals in subcellular neuronal compartments, including spines and varicosities, with high spatial and temporal resolution [5]**.** For such subcellular measurements, made from structures deep in intact, highly scattering tissue like the CNS, MPE microscopy is still the major technique of choice and has contributed to several major discoveries [8].

When imaging Ca^{2+} signals and dynamics in subcellular neuronal compartments, it should ideally be possible to apply stimuli with the same degree of spatial and temporal resolution as is possible for recording the Ca^{2+} signal itself. In some cases, action potentials triggered by extracellular stimulation of axons can evoke Ca^{2+} signals that lead to presynaptic release of neurotransmitter onto the postsynaptic target. With adequate placement of the stimulation electrode, it is possible to activate single axons [9]. Alternatively, extracellular stimulation can be used to depolarize non-spiking neurons to the threshold for releasing neurotransmitter [10]. In the latter case, it is difficult to ensure single-synapse stimulation and the specificity may be suboptimal. In some situations, it is possible to record intracellularly from a presynaptic neuron and use this to trigger release at specific synapses, but with whole-cell recording there is often a rapid rundown of release (especially with small neurons). In situations where presynaptic activation is not an option (either because of technical limitations or because desired pharmacological manipulations of postsynaptic mechanisms interfere with or compromise presynaptic release), it may be possible to directly activate postsynaptic receptors by agonist application. Ideally, however, the method of application should be designed to mimic the spatial and temporal aspects of normal synaptic activation. That is, the method should, as far as possible, enable activation of a single postsynaptic structure and the time course of activation of receptors should be similar to that experienced during presynaptic release. Fine-tipped glass micropipettes, e.g. the sharp microelectrodes used for intracellular recording, are sufficiently small and can be used for drug application within a sufficiently small region [11, 12], using either iontophoresis or pressure. The challenge, however, is to target the application to specific, visually identified subcellular structures and to ensure that the speed of application is sufficiently fast. Pressure application causes mechanical disturbances that can compromise Ca^{2+} imaging. In addition, if the pipette tip is not sufficiently small, leakage of the substance can make it problematic to position the tip close to the target. A larger distance between the pipette and the target compromises the speed and spatial restriction of application. A smaller tip size can make it difficult to use pressure

ejection. Many of these problems can be avoided with microiontophoresis, where the agonist (or any other charged solute) can be ejected in a very small amount from a fine-tipped glass micropipette. With such pipettes and conventional microiontophoresis, leakage of substance can be further reduced to a minimum by applying a retaining current. However, the high pipette resistance in combination with the pipette capacitance acts as a low-pass filter that seriously compromises the speed of application. Prolonging the duration of the stimulus will compromise not only the temporal control, but also the spatial resolution and specificity of the application. One solution to these challenging problems has been to fully compensate the capacitance of the high-resistence glass micropipette, reducing the effective pipette time constant and thereby enabling application of agonist with a time course that, in the best cases, mimics the time course of synaptic release [13, 14]. This technique was initially applied to neurons in cell cultures where the conditions for high-resolution visualization are particularly favourable, but has recently been successfully applied to neurons in *in vitro* CNS slice preparations [6, 15, 16]. When the goal is to use fast microiontophoresis to apply agonists to study subcellular Ca^{2+} dynamics with MPE microscopy, concomitant structural imaging allows visual targeting of the specific subcellular compartments of interest. Structural imaging is also extremely useful for accurate positioning of a microiontophoresis pipette, also for studies where the primary goal is to investigate e.g. the subcellular localization and function of neurotransmitter receptors by electrophysiological recording. Here, we provide a detailed description of experimental procedures for the combination of fast microiontophoresis, electrophysiological whole-cell recording, and structural and functional MPE microscopy applied to *in vitro* slice preparations from CNS tissue, together with examples of experimental results that can be obtained.

2 Materials and General Methods

2.1 Animal Anaesthesia

All work with animals must be approved and performed in accordance with local

(institutional) and national regulations. Deeply anaesthetize the experimental animal (e.g. a rat or a mouse) with isoflurane (~2 to ~3%) in oxygen. Use 100% oxygen as opposed to ordinary air, as this strongly reduces the risk of laryngeal spasms and consequent hypoxia that compromises tissue quality. When an adequate depth of anaesthesia has been reached, kill the animal by cervical dislocation or decapitation.

Fig. 1 near here

2.2 In vitro Slice Preparation

Depending on the region of the central nervous system from which the slice preparation will be made, different procedures for cutting the slices will have to be applied. The procedure described here is from our laboratory where the work is focused on the mammalian retina. After removing the eyes, rinse the eyes briefly in cold dissection solution (for details, see [16] and references therein). With the eyeball immersed in solution, locate it under a dissection microscope and use fine forceps and a scissor to remove extraocular connective and muscle tissue from the eyeball. Open the eyeball with a syringe needle, and use a small scissor to make an encircling cut slightly posterior to the ora serrata. Remove the front half corresponding to the cornea, lens and the bulk of the vitreous body. Use fine forceps to thoroughly, but gently remove any remaining pieces of vitreous. Gently dissect the retina from the rest of the eyeball. Divide the retinal eyecup into four quadrants and store them on small pieces of lens paper on top of a nylon mesh in an interface chamber with Ames solution (Sigma A1420) buffered (pH) by addition of $NaHCO_3$ and bubbling with gas containing 5% CO_2 (and 95% O_2). Cut retinal slices (at a thickness of 100 - 200 μm) by hand under a dissection microscope by using a curved scalpel blade. Alternatively, embed pieces of retina in low-temperature gelling agar (Sigma A0701) and cut slices from the agar block with a vibrating microtome (e.g. Leica VT1200). This kind of vibratome is the instrument of choice for cutting high-quality slices directly from trimmed tissue blocks from other regions of the CNS (e.g. hippocampus, thalamus, brain stem, etc. [17]), including slices suited for axon terminal and dendritic recordings

[18, 19]. A single set of slices should not be used for more than 3 - 4 hours before being replaced by a new set.

2.3 Visualization with Dodt Gradient Contrast Videomicroscopy and MPE Microscopy

After preparing *in vitro* slices from a specific CNS region, place the slices in a perfusion or recording chamber (Fig. 1a) and secure them by gently placing a U-shaped "harp" (made from platinum-iridium wire) with thin nylon wires glued on one side. Place the chamber under the microscope to visualize the slices (Fig. 1b). For our experiments, we use a custom-modified "Movable Objective Microscope" (MOM) from Sutter Instrument (https://www.sutter.com) equipped with e.g. a ×20 water immersion objective (XLUMPLFL, 0.95 NA; Olympus). All of the major microscope manufacturers offer MPE microscopes, typically modified confocal microscopes, that provide similar functionality. Some laboratories have designed their own MPE microscope (see chapter by Smith, this volume) and there are several published designs available, although the level of detail differs [20]). To adequately visualize the slices, it is necessary to employ some form of contrast enhancement. Infrared (IR) videomicroscopy works well with differential interference contrast (DIC; Nomarski), but the optical elements for DIC are difficult to combine with fluorescence microscopy without losing substantial signal intensity [21]. Instead, we use IR Dodt gradient contrast (IR-DGC) videomicroscopy [9, 22] with hardware from Luigs & Neumann (http://www.luigs-neumann.com) and a standard IR-sensitive analog CCD camera (e.g. VX55 from TILL Photonics). Powerful light-emitting diodes (LEDs) can be a convenient source for IR light. One example, with peak intensity around 780 nm, is the LED M780L2 from Thorlabs (https://www.thorlabs.com).

2.4 Patch Pipettes for Electrophysiological Recording

Patch pipettes should be made from thick-walled borosilicate glass, e.g. with outer diameter of 1.5 mm and inner diameter of 0.86 mm (Fig. 1c). There are several

companies that supply high-quality glass for pulling pipettes (e.g. Sutter Instrument and WPI [https://www.wpiinc.com]). For pulling patch pipettes, it is necessary to use a two-stage puller (e.g. PC-100 from Narishige [http://uk.narishige-group.com], PIP 6 from HEKA Elektronik [http://www.heka.com] and P-97 or P-1000 from Sutter Instrument). For easier filling of the tip of the pipette with intracellular electrolyte solution, we recommend using filamented glass. Depending on the type of cell the recording will be made from, the open-tip resistance of the pipette (when filled with intracellular solution and positioned in the extracellular bath solution) can range from about 4 to 12 MΩ.

2.5 Intra- and Extracellular Solutions

The extracellular bath solution should be continuously bubbled with 95% O_2-5% CO_2 for oxygenation (which is required when working with slice preparations of vascularized CNS tissue to compensate for the increased diffusion distance after termination of capillary circulation) and pH control (CO_2 / bicarbonate buffer system). A standard extracellular solution can have the following composition (in mM): 125 NaCl, 25 $NaHCO_3$, 2.5 KCl, 2.5 $CaCl_2$, 1 $MgCl_2$, 10 glucose, pH 7.4. If the experimental design requires heating above room temperature, appropriate instrumentation is required for heating the bath solutions and the recording chamber (e.g. Warner TC-324C; https://www.warneronline.com).

Depending on the experimental design, the recording pipettes can be filled with a solution of the following composition (mM): 125 potassium gluconate, 8 NaCl, 5 KCl, 10 Hepes, 0.2 EGTA, 4 magnesium ATP, and 0.4 disodium GTP. pH is adjusted to 7.3 with KOH. When required, EGTA can be replaced with the faster Ca^{2+} buffer BAPTA [23]. For structural MPE imaging, we add Alexa Fluor 488 hydrazide or 594 hydrazide (both as sodium salts; Thermo Fisher / Invitrogen A10436, A10438) to the pipette solution for visualization of the cellular morphology. Depending on the cell size (including the length of the relevant processes and the distance from the soma to the

targeted structures), recommended concentrations are in the range of 20 to 60 μM. Higher concentrations can result in excessive spill or pooling of dye around the site of recording. It is also important to check the osmolality of the solution. Values in the range of 290 - 300 mOsm/kg are adequate for slices from rat CNS, but other species may require moderately different values.

For MPE microscopic Ca^{2+} imaging, the recording pipettes can be filled with the same solution, but EGTA (or BAPTA) is replaced with an appropriate Ca^{2+} indicator, e.g. Oregon Green 488 BAPTA-1 (OGB-1; 200 μM; Thermo Fisher / Invitrogen) or another indicator with different Ca^{2+} affinity [9]. When the intracellular solution contains dyes for structural and/or functional imaging, it is useful to prepare a stock solution at ×1.25 of the final concentration without fluorescent dyes, filtered to remove particles that can obstruct the recording pipettes (e.g. 0.22 μm syringe filters from Millipore; SLGV004SL) and stored at -20°C until use. Before the experiment, the ×1.25 stock solution is diluted with water and/or fluorescent dye(s) dissolved in water to the appropriate concentration. A stock solution of fluorescent dye can be made by dissolving it in water (Sigma W3500) at a concentration of 1 mM and storing it as 100 μl aliquots at -20°C until use. To conserve expensive dyes for structural and functional imaging, we make up a small volume (20 μl) of intracellular solution (at ×1 concentration) and fill each recording pipette with as little as 1 - 2 μl of solution. With such small total volumes, the pipettes can conveniently be filled by using long plastic tips (e.g. Eppendorf Microloader tips).

2.6 Electrophysiological Recording and Data Acquisition

Whole-cell recordings are performed with a high-quality patch-clamp amplifier (e.g. the EPC10 series from HEKA Elektronik and the dPatch from Sutter Instrument). Depending on the design of the amplifier, it can either be integrated with the other components required for amplifier control and data acquisition or be connected to an

independent device for data acquisition with analog-to-digital and digital-to-analog signal conversion. Some systems come with integrated software (e.g. Patchmaster from HEKA Elektronik and SutterPatch from Sutter Instrument). Some laboratories write their own software for amplifier control and data acquisition (e.g. in the IGOR Pro environment; https://www.wavemetrics.com).

After establishing a GΩ-seal, currents caused by the recording electrode capacitance (fast capacitive current) should be measured and neutralized by the amplifier, either manually or automatically. After breaking into the cell and establishing a whole-cell recording, currents caused by the cell membrane capacitance (slow capacitive current) should also be measured and (fully or partially) neutralized by the amplifier, either manually or automatically.

For ordinary electrophysiological responses, it is usually adequate to low-pass filter (analog or digital Bessel filters) the signals with a cut-off (corner) frequency (f_c; -3 dB) in the range between 1 and 4 kHz. The sampling interval should ideally be the inverse of $5 \times f_c$, at most the inverse of $2 \times f_c$ (to satisfy the Nyquist criterion for digital sampling). If it is desirable to also sample the very brief stimulus signals used for microiontophoretic application (see below) for documentation purposes, it is necessary to use a correspondingly short sampling interval, e.g. 10 μs.

2.7 MPE Microscope

In our system, we switch from IR-DGC videomicroscopy to MPE microscopy by changing the optical paths of the MOM via movable mirrors. In the MOM, scanning is performed by galvanometric scanners (MicroMax 673XX dual axis; Cambridge Technology, https://www.cambridgetechnology.com), equipped with either 3 or 6 mm mirrors (6210H; Cambridge Technology). The smaller mirrors are preferred for faster imaging, whereas the larger mirrors are preferred for higher resolution (as the expansion of the laser beam can be increased). To maximize the spatial resolution, the

laser beam should be expanded (before hitting the scanning mirrors) such that it overfills the back aperture of the microscope objective [24]. The intensity of the laser is typically so high that the corresponding loss of light never poses a problem. Our setup is equipped with a computer-controlled, mode-locked, ultrafast-pulsed Ti:sapphire laser with tunable wavelength (690 - 1040 nm; Mai Tai HP Deep See; Spectra-Physics; https://www.spectra-physics.com). To minimize the total exposure time of the preparation during image acquisition, the laser light should be controlled by a high-speed laser shutter (e.g. LS6ZM2 from Vincent Associates; https://www.uniblitz.com). To attenuate the intensity of the laser, and thus control the exposure of the preparation to the laser light, it is useful to include an electro-optic modulator (EOM; "Pockels cell") in the optical pathway. A specific advantage of an EOM is that it has an extremely fast response time (≤1 μs rise/fall time). We use the "350-80LA with BK option" from ConOptics (https://www.conoptics.com). An EOM is driven by an external amplifier that should be controlled by the MPE acquisition software / hardware system. We use the 302RM amplifier from ConOptics.

The emitted epifluorescence light for MPE imaging and the forward-scattered laser light for IR-laser scanning gradient contrast (IR-LSGC) microscopy (see below) are detected by separate photomultiplier tubes (PMTs). Our system is equipped with multialkali PMTs (R6357; Hamamatsu; https://www.hamamatsu.com). There are other alternatives for PMTs, including the more sensitive GaAsP-based detectors (e.g. H10770PA-40; Hamamatsu). The analog signals from the PMTs are digitized by a fast acquisition board (e.g. NI-6110E from National Instruments; http://www.ni.com).

2.8 Computer Software for MPE Microscopy

MPE microscopy and image acquisition is controlled by dedicated computer software. Commercial MPE microscopy systems typically come with custom software sold by the microscope manufacturer. Alternatively, there are software programs, typically originating from academic research environments, that have been developed as generic

programs with sufficient flexibility that they can be adapted to different microscope systems with a range of hardware components. The most commonly used programs are ScanImage ([25]; http://scanimage.vidriotechnologies.com; https://vidriotechnologies.com), HelioScan ([26]; http://helioscan.github.io/HelioScan) and MPScope ([27]; https://neurophysics.ucsd.edu/software.php). Our system is controlled by ScanImage software (version 3.8 and higher; developed under MATLAB; MathWorks, https://www.mathworks.com). This program digitizes the image data at 12-bit resolution and stores the files as 16-bit TIFF files.

2.9 Pipettes for Microiontophoresis in in vitro Slice Preparations

For high-resolution microiontophoresis [13-16] with spatially and temporally restricted activation of e.g. glutamate receptors on subcellular neuronal structures, it is necessary to use fine-tipped micropipettes with high resistance. This is necessary to match the dimensions of the relevant structures (e.g. small varicosities and thin dendritic processes), to minimize tissue damage, and to reduce the passive diffusion (leakage) of agonist (and dye; see below) from the pipette tips. Pipettes with resistances in the range between 90 and 120 MΩ perform well and can be pulled in two stages on a horizontal puller (in our case, the Flaming Brown P-97 pipette puller; Sutter Instrument).

Traditionally, the way to prepare micropipettes with such high resistances is to use thin-walled glass designed for sharp microelectrodes and intracellular recording (e.g. outer diameter, 1.0 mm; inner diameter, 0.78 mm). Such pipettes can work well when applied to cells in tissue culture [13, 14]. However, in our experience, using a slice preparation, such pipettes only work well for targeting visually identified structures located a few μm below the surface of a slice. For deeper structures, the tips of these pipettes are too flexible and tend to bend and thus deviate from their trajectory inside the tissue before reaching the target. To produce pipettes with stiffer tips, we instead

use the same thick-walled glass used for patch pipette recording (filamented borosilicate glass; outer diameter, 1.5 mm; inner diameter, 0.86 mm). With such glass, we are able to prepare pipettes with long thin tips that do not bend when inserted into the neural tissue and have sufficiently high resistance that leakage of drug can be controlled with acceptable retaining currents (Fig. 1c, and see below). It is important that the pipettes are pulled such that the distance from the tip to the wider shaft (i.e., the taper) is sufficiently long to avoid compression of the tissue when inserted into the slices. Shorter tapers will increase the relative instability between the pipette and the tissue and lead to slow spatial drift ("relaxation") between tissue and pipette after positioning the pipette close to a given subcellular structure. The extent to which this is a problem is likely to vary with the mechanical properties of the tissue, related to the specific region of the CNS from which the *in vitro* slices are prepared. We have designed our pipettes with inspiration and guidance from the Sutter Instrument Pipette Cookbook (https://www.sutter.com/PDFs/pipette_cookbook.pdf; see Table 1 for specific parameters). The parameters ("velocity" and "time") that we regularly tweak to obtain desired resistances are provided as ranges.

Some authors have suggested that iontophoresis micropipettes can be re-used between experiments, especially desirable with pipettes that perform particularly well. To enable such re-use, it is important to store the micropipette in a closed container with a humidified atmosphere to prevent drying out and clogging at the tip. For certain drugs, it is also necessary to protect the pipette solution from light. In our experience, we have not found it worthwhile to re-use pipettes between experiment days, but we generally use the same pipette during the course of an experiment day.

Table 1 near here

2.10 Pipette Solutions for Microiontophoresis

Depending on the receptors to be activated by microiontophoresis, the pipettes can be

filled with L-glutamate, L-aspartate, NMDA, GABA, etc. The concentration of the drug must be sufficiently high (both in absolute and relative terms) such that it will carry a substantial part of the total current applied during iontophoresis [11], but sufficiently low such that leakage from the tip of the micropipette does not become excessive. For the relevant drug molecules to be able to carry current, the pH of the solution must be such that the molecules exist in an ionized form. For glutamate, we have good experience with a concentration of 150 mM (in water) and pH adjusted to 7.0 (with NaOH). Additional examples can be found in [15].

For a typical micropipette with a resistance of 90 to 120 MΩ, the spatial resolution of light microscopy is insufficient to visualize and resolve the true size of the pipette tip (Fig. 1c; [28]). For visualization of the pipette tip during MPE microscopic imaging, a fluorescent dye (e.g. Alexa 594) must be added. This is also very useful for tuning the retaining current, verifying the ejection, and targeting the pipette tip to a specific subcellular structure of a neuron during MPE microscopy. It makes sense to use the same dye for structural imaging of both the neuronal processes and the microiontophoresis pipette. In our experience, a pipette concentration of 40 μM for Alexa 594 is a good balance between adequate visualization and potential leakage that might interfere with structural imaging of neuronal processes. For experiments that do not combine electrophysiological recording with imaging using a Ca^{2+} indicator with green fluorescence, Alexa 488 could be used instead of Alexa 594, but in our experience, Alexa 594 yields brighter fluorescence for a given concentration of dye.

2.11 Microiontophoresis Amplifier for fast Drug Application

When the goal is to apply very brief pulses of a drug (e.g. < 1 ms), it is necessary to use an amplifier for current injection that enables electronic compensation of the capacitance of the microiontophoresis pipette. With no or insufficient compensation, a brief current pulse will only charge the pipette capacitance instead of ejecting drug. Increasing the duration of the current pulse will eject drug, but leads to reduced spatial

and temporal resolution of the application. To our knowledge, there is currently only one commercially available system that allows for electronic compensation of the pipette capacitance, made by NPI Electronic (http://www.npielectronic.de). This company offers several variants of a basic design and our experience is with the MVCS-C-02M system that allows application speeds that can simulate brief synaptic events. In the high-voltage version (up to ±225 V), it allows application of currents up to ±2.25 μA (into a 100 MΩ resistance), with positive or negative polarity set according to the charge of the molecule to be ejected. The MVCS-C-02M system allows capacitance compensation in the range 0-30 pF and maximum retaining currents of ±100 nA.

Fig. 2 near here

2.12 Capacitance Compensation and Tuning of Pipettes for fast Microiontophoresis

As stated above, ejecting a substance by iontophoresis using current pulses in the submillisecond range (0.5 - 1 ms) depends crucially on the ability to adequately compensate the capacitance of the pipette. It is also necessary to adequately compensate the capacitance before the pipette resistance can be measured correctly. Because the effective capacitance of the micropipette will be related to the extent of immersion in the fluid of the recording chamber, the fluid level should be kept as low as possible. Capacitance compensation and resistance measurement should be first performed with the micropipette in the bath, but before insertion into the tissue, and should be verified several times throughout an experiment. Compensation of the capacitance of a microiontophoresis pipette is illustrated in Fig. 2, with application of repeated current pulses of ±10 nA (5 ms duration). The illustrated capacitance settings correspond to an under-compensated pipette, a correctly and accurately compensated pipette, and an over-compensated pipette, respectively. If the fluid level of the recording chamber does not change during the experiment, it is not expected that the capacitance will change. We have not attempted to reduce the pipette capacitance by coating it (e.g. with silicone elastomer, dental wax or Parafilm) as this is likely to

interfere with the movement of the pipette in the neural tissue and cause instability of its position relative to the tissue. When the capacitance has been correctly compensated, the resistance can be directly calculated from the amplitude of the voltage deflection in response to the applied current, using Ohm's law. It can be useful to check the resistance of the pipette multiple times during the recording to ensure the tip is not clogged.

In addition to compensating the capacitance of the microiontophoresis pipette, we have also found it necessary to perform a procedure that "primes" the pipette before it is inserted into the neural tissue. For application of glutamate (as an example), this involves repeatedly passing current pulses of negative polarity (e.g. ≤ -200 nA for 200 ms; 2-3 Hz) for 3-6 minutes to eject and optimally fill the tip of the pipette with glutamate (and fluorescent dye). The result of this priming is that the pipette tip is optimally visualized and that subsequent application of current pulses (of the correct polarity) will evoke precise and efficient ejection. This procedure should be performed while the tip of the pipette is in the bath solution, well above the tissue surface, and can be monitored by continuous MPE microscopy while focusing on the tip of the pipette. With the iontophoresis solution employed here, Alexa 594 is ejected by the same current polarity as glutamate (i.e., with negative current). We do not fully understand the mechanism underlying the "priming" phenomenon, but it has been suggested that current pulses of alternating polarity can serve to remove small air bubbles inside the pipette tip [29].

After successful priming of a pipette, it is relatively straightforward to adjust the retaining current (using the polarity opposite to that used for ejection) such that there is neither visible leakage of dye nor depletion of dye from the tip of the pipette. This procedure is performed with MPE microscopic imaging (see below) at high zoom while one attempts to focus as closely as possible at the expected position of the tip of the micropipette. When the retaining current is optimally adjusted, the MPE

microscopic image of the pipette tip will correspond to the longest possible tip, with an optimal balance between the retaining current being too low (observed as an apparent shortening of the tip caused by leakage and consequent dilution of dye from the tip) and the retaining current being too high (observed as an apparent shortening of the tip caused by retraction of dye from the tip. For experiments with the glutamate-filled pipettes described here, we typically apply a retaining current in the range of +10 to +20 nA. If necessary, this current can be adjusted once the pipette has been positioned close to the targeted subcellular structure. If electrophysiological recording is performed simultaneously from the targeted neuron, leakage of glutamate can potentially be detected as an increase of current (or voltage) noise.

2.13 MPE Microscopy for Structural and Functional Imaging

In general, both Alexa Fluor 594 (20 - 60 μM) and Alexa Fluor 488 (50-60 μM) can be used for structural MPE imaging with good results. The wavelength of the laser is optimally tuned to 775 nm for Alexa 488 and to 810 nm for Alexa 594. We use the latter wavelength for simultaneous imaging with Alexa 488 and Alexa 594 (e.g. for simultaneous, dual recording and imaging of two neurons filled with different dyes) and also for cells filled with both Alexa 594 and the green fluorescent Ca^{2+} indicator OGB-1.

For acquisition, we usually sample two fluorescence channels, red fluorescence from Alexa 594 added to the solutions in the recording and microiontophoresis pipettes for structural imaging and green fluorescence (e.g. from OGB-1 added to the recording pipette) for functional imaging. In addition, we sample a third channel for IR-LSGC microscopy. The latter channel samples images using the forward scattered laser light after it passes the substage condensor and a Dodt gradient contrast tube in reverse [9].

For structural imaging, we generally acquire image stacks as a series of optical slices (512 × 512 or 1024 × 1024 pixels; typically with averaging of two frames for each slice) at constant focal plane intervals (e.g. 0.4 μm). For imaging intracellular Ca^{2+}

dynamics, we sample fluorescence from relevant subcellular structures, either as high-speed line scans (e.g. with 64 pixels/line and temporal resolution of ~960 Hz) or as lower-speed frame scans (e.g. 16 × 16 pixels at ~25 Hz or 32 × 32 pixels at ~14 Hz). To synchronize Ca^{2+} imaging and electrophysiological recording, we use a digital output from the patch-clamp amplifier to trigger image acquisition (with ScanImage).

Fig. 3 near here

2.14 Structural Imaging for Targeted Microiontophoresis

The neurons and structures of interest can be targeted based on their location in the tissue, details of the cellular morphology and/or expression of specific fluorescent proteins (see chapter by Chen and Wei, this volume). In the examples used here, cell bodies of amacrine and bipolar cells in the mammalian retina can be identified based on their location in the inner nuclear layer and the specific morphology of cell bodies and proximal processes (Fig. 3). AII amacrine cells are targeted based on the position of a cell body at the border of the inner nuclear layer and the inner plexiform layer with a thick primary dendrite that descends into the inner plexiform layer (Fig. 3a). Bipolar cells are targeted based on their location in the outer and middle parts of the inner nuclear layer (Fig. 3b). A17 amacrine cells are targeted based on the location of a dome-shaped cell body (with the base towards the inner plexiform layer) at the border of the inner nuclear layer and inner plexiform layer (Fig. 3c).

Structural imaging with MPE microscopy is essential for identifying and targeting the subcellular structures of interest, both for microiontophoretic application combined with electrophysiological recording and for the addition of functional Ca^{2+} imaging. MPE microscopy is eminently suited to identify complex neuronal structures at high resolution with a low risk of phototoxicity that allows for long-lasting imaging. During the initial phase of a recording experiment, the limiting factor is the diffusion of the dye used for structural imaging. Diffusion from the pipette into the soma is rapid, but sufficient diffusion from the soma into the (distal) dendritic tree depends on the size

and structure of the cell (including the length and thickenss of the processes), and can take considerable time. For small neurons like AII amacrine cells (Fig. 3d) and bipolar cells (Fig. 3e, f) it is not necessary to wait more than 10-15 min after establishing the whole-cell configuration before commencing either microiontophoretic targeting and/or functional imaging. For neurons with large dendritic trees and thinner processes (e.g. A17 amacrine cells), it is typically necessary to wait at least 30 min such that the structural dye and/or the Ca^{2+} indicator has reached the desired subcellular neuronal compartments at a sufficient concentration (Fig. 3g). During this period there is ample time to use short periods of MPE imaging to verify the identity and condition of the neuron and to add pharmacological blockers and verify their action (by electrophysiological recording).

2.15 Targeting the Microiontophoresis Pipette to Specific Subcellular Structures

When using fast microiontophoresis to apply a drug to a specific and visually identified subcellular structure, the goal is to position the tip of the micropipette as closely as possible to the neuronal structure to make sure, to the largest extent possible, that any measured response originates from the targeted structure. Because the tip of a micropipette with a resistance in the range of 90 - 120 MΩ is extremely small, this can be quite challenging (see Fig. 1c). We have never measured the diameter of the tip of our pipettes used for microiontophoresis, but from general experience, pipettes with this resistance typically have diameters in the range of 0.05 μm when imaged by scanning electron microscopy [28]. Because this is below the limit of resolution of light microscopy, it means that we cannot know the true position of the pipette tip. Filling the pipette with a fluorescent dye and imaging the tip with MPE microscopy is a potential solution to this problem. When the pipette is filled all the way to the tip with fluorescent dye at a concentration sufficiently high to give a detectable signal, it is in principle possible to identify the location (but not the diameter) of the pipette tip with MPE microscopy.

Fig. 4 near here

For targeting the tip of the microiontophoresis pipette to a specific subcellular structure below the surface of the slice, we monitor both the dye-filled cell and the dye-filled pipette tip with MPE microscopy. For precise targeting, we have found it useful to follow a fixed procedure in which distances are estimated as accurately as possible. The main difficulty with a less stringent procedure is that once the micropipette is inside the slice, it is essentially impossible to move the pipette sideways to compensate for an inaccurate initial position. The following procedure (Fig. 4) depends on the MPE microscope being equipped with a motorized focus drive to accurately measure the distance between focal planes with μm resolution. It also depends on having access to a motorized three-axis micromanipulator where the X-axis corresponds to the long axis of the microiontophoresis pipette, the Y-axis is horizontal and oriented 90° degrees to the X- and Z-axes, and the Z-axis is vertical and oriented 90° to the Y-axis (e.g. the Mini25 from Luigs & Neumann). In our setup, the angle between the long axis of the pipette (X-axis) and the horizontal plane is 20°. This shallow angle is determined by the use of a water immersion objective for visualization of the slice preparation and the need to position the pipette between the slice and the objective. The objective used in our setup (x20 XLUMPLFL; 0.95 NA; Olympus) is particularly wide, but similar objectives have been designed with a more pointed front that might allow a steeper angle of the pipette to be used.

With continuous visualization by MPE microscopy, proceed as follows:

1. Using a displayed crosshair (XY) as a reference in the imaging software, position the targeted subcellular structure at the center of the crosshair.
2. Position the tip of the microiontophoresis pipette above the slice (20 - 30 μm) such that it touches the center of the crosshair (XY) and thereby is superimposed vertically with the targeted subcellular structure (Fig. 4a; corresponding to position 1 in Fig. 4b).
3. By changing the focal plane between the target structure (focal plane Z_1 in Fig. 4a) and the tip of the pipette (focal plane Z_2 in Fig. 4a), measure this distance as accurately

as possible. This distance is indicated in Fig. 4b as *a*+*b*, where *a* is the distance between the pipette tip and the slice surface and *b* is the distance between the slice surface and the target structure.

4. Move the pipette a distance *c* (marked red in Fig. 4b) outwards from the center of the field of view along its long axis (the X-axis), corresponding to position 2 in Fig. 4b. The pipette will now be outside the field of view.

5. Move the pipette downwards the same distance *a*+*b* along the Z-axis, corresponding to position 3 in Fig. 4b. This is done "blindly", with the pipette outside the field of view.

6. Move the pipette inwards the same distance *c* that it was moved outwards (in step 3 above) along its long axis (X-axis), corresponding to position 4 in Fig. 4b. For optimal control, the digital zoom of the MPE microscopic image should be decreased during the initial part of the movement to bring the pipette into the field of view and then gradually increased as the tip of the pipette approaches the targeted structure. In this way, the tip of the pipette can be detected as it enters the slice (or shortly thereafter) and visually tracked (with increasing digital zoom) on its way to the targeted structure.

In our experience, when performed with high-resolution micromanipulators, this procedure is successful in accurately positioning the pipette tip without requiring any re-positioning (Fig. 4c). In some cases, the final position will deviate along the Y-axis ("north / south" as displayed in the imaging software) and/or along the Z-axis (vertical; Fig. 4d). In such cases, the spatial offset (along the Y axis and/or Z axis) can be estimated before moving the pipette out of the tissue. Then the pipette can be re-positioned to compensate for the offset and moved back in again along the X-axis. The crucial part of the procedure is the retraction distance *c* that the pipette is moved outwards in step 4 above. If *c* is too short, the tip of the pipette will hit the surface of the slice as it is moved downwards in step 5. A simple geometrical analysis indicates that for the conditions used here, *c* should be (at least) ~3 times the distance *ab*. In this case, the pipette tip will be a distance *a* above the tissue surface in position 3, with the distance *c* equal to $ab/\sin\alpha$, or approximately $3ab$ for $\alpha = 20°$, as in our case.

Accordingly, a multiplication factor of 3 - 3.5 should be sufficient to ensure that the tip of the pipette does not bump into the slice when moved downwards to position 3 (Fig. 4b). If the slice surface is very uneven, a larger factor can be used for calculating the retraction distance *c*. Depending on the experiment, it can be a good idea to check the capacitance compensation of the microiontophoresis pipette again after it has been moved into the tissue and is 20 - 30 μm away from the target structure.

Fig. 5 near here

2.16 Electrophysiological and Intracellular Ca^{2+} Responses Evoked by Fast Microiontophoretic Application of Agonist

The charge of the drug molecules in the solution of the microiontophoresis pipette will determine whether they can be ejected by applying a positive or a negative current (see [11, 12, 15] for other examples). The examples discussed here use application of glutamate to subcellular structures of AII and A17 amacrine cells in the rat retina.

After the tip of the microiontophoresis pipette has been positioned close (1 - 2 μm) to the structure of interest under visual control using MPE microscopy (Fig. 4), glutamate can be ejected by application of negative current pulses (typically -200 to -600 nA). When the capacitance of the microiontophoretic pipette has been adequately compensated (see Section 2.12), even very brief current pulses can evoke responses that can be detected in whole-cell recordings. Figure 5 illustrates a response evoked in an A17 amacrine cell (Fig. 3g) by a brief current pulse (-500 nA, 1 ms) when the microiontophoretic pipette was positioned close to a dendritic varicosity (Fig. 5a) where these cells receive synaptic input from glutamatergic rod bipolar cells [30]. Application of glutamate evoked a transient inward current (Fig. 5b) immediately after the iontophoretic current pulse. The rise times observed for such responses evoked in voltage-clamp recordings will typically be slower than the fastest rise times observed for spontaneous excitatory postsynaptic currents (spEPSCs). Because spEPSCs essentially can arise anywhere in the dendritic tree, it will only rarely be possible to

directly compare their rise times with those of responses evoked by microiontophoresis at a specific location. In addition, it is unlikely that the temporal concentration profile of agonist applied iontophoretically in intact neural tissue can completely mimic that of neurotransmitter released in synapses. Even if the speed of ejection from the tip of the micropipette could match that of release from synaptic vesicles fusing with the plasma membrane of the presynaptic neuron, the diffusion distance to the receptors in the postsynaptic density will inevitably be larger than the corresponding distance in the synaptic cleft.

When structural MPE imaging, microiontophoretic drug application and electrophysiological recording (voltage clamp or current clamp) are combined with functional MPE imaging of intracellular Ca^{2+}, it is important to allow sufficient time for the Ca^{2+} indicator dye to diffuse into the target structure and reach a relatively stable concentration, thereby reducing a potential source of response variability. The increase in intracellular Ca^{2+} can be measured by using either line scans or frame scans, depending on the application and the temporal resolution required. Line scans sacrifice spatial information in favour of achieving higher temporal resolution (compared to frame scans). However, the advantage of higher temporal resolution must be considered in relation to the higher sensitivity to small changes in the position of the relevant subcellular structure caused by drift and instability. For applications where the goal is to quantify changes in the Ca^{2+} response over time in response to various experimental manipulations, frame scanning is preferred over line scanning.

As described earlier, line scans and frame scans of the target structure(s) must be precisely synchronized with the current stimulus applied to the microiontophoresis pipette and the electrophysiological recording. In our laboratory, we have found it most convenient to initiate data acquisition from the electrophysiological setup and use digital and/or analog output signals to trigger image acquisition and application of the microiontophoretic current. It can be a considerable challenge to keep track of the

correlation between epochal image data and electrophysiological data during off-line analysis. For systems where the two types of data are saved in separate computer files, off-line analysis critically depends on recording the exact times of acquisition for both sets of data. It is common to use separate computers for hardware control and data acquisition for imaging and electrophysiology and it is important to ensure that the date and time of the two computers are synchronized. Some programs for MPE imaging allow correlated electrophysiological data to be saved in a separate channel of the imaging data file [27].

Figure 5c illustrates a Ca^{2+} response obtained by MPE imaging performed in parallel with the electrophysiological recording (Fig. 5b) during microiontophoretic glutamate application to the A17 dendritic varicosity. For this A17 amacrine, Ca^{2+} imaging started ~30 min after establishing the whole-cell configuration to allow for maximal indicator loading at distal varicosities.

Ca^{2+} signals can be analyzed using standard procedures, with measurement of background fluorescence (F_b) as the average signal from a rectangular area close to the region of interest and baseline fluorescence (F_0) by averaging the signal in the region of interest during an interval before stimulus onset. For a given signal (F), the relative change in fluorescence related to a change in Ca^{2+} is then calculated as [9]:

$$\frac{\Delta F}{F_0} = \frac{F - F_0}{F_0 - F_b}$$

This equation is often referred to simply as $\Delta F/F$.

Fig. 6 near here

If we assume that the observed responses are generated by ejection of drug and activation of receptors in the membrane of the postsynaptic cell (in contrast to indirect effects mediated e.g. by the electrical stimulation activating synaptic release of neurotransmitter from neighboring neurons; see Section 2.18), that the ejected amount of drug does not saturate the receptors, and that the increase of intracellular Ca^{2+} does

not saturate the indicator dye, it should be possible to increase both the electrophysiological and Ca^{2+} responses by ejecting a larger amount of drug. This can be achieved by increasing either the amplitude and/or the duration of the current used for ejection. For the example illustrated in Fig. 6, the ejection current was varied from 0 to -500 nA in steps of -100 nA while the duration was kept constant at 1 ms. The evoked electrophysiological (Fig. 6a) and Ca^{2+} responses (Fig. 6 b) increased in parallel with increasing stimulus intensity (Fig. 6c). The ability to establish tentative dose-response relationships like these, suggests that the system is within its dynamic range and does not saturate for the range of stimuli applied. A more detailed examination is difficult, however, as the drug concentration in the vicinity of the receptors is essentially unknown. It is a consistent observation that electrophysiological responses such as the ones illustrated here can be maintained for longer periods of time than the corresponding intracellular Ca^{2+} responses. This could be related to a gradually developing phototoxicity that is unavoidable with functional imaging and/or the susceptibility of intracellular signal transduction mechanisms (involved in generating Ca^{2+} responses) to rundown.

Fig. 7 near here

2.17 Estimating the Spatial Profile of Glutamate After Microiontophoretic Ejection

One important reason for employing very brief pulses during microiontophoretic drug application is to limit the spatial extent of receptor activation. One way to investigate the spatial extent of activation is to examine how the evoked response changes as a function of the position of the microiontophoretic pipette as the pipette is gradually retracted from the targeted subcellular compartment. Figure 7 illustrates the results from an experiment where we targeted a specific dendritic varicosity of an A17 amacrine cell (Fig. 7a) and measured the voltage-clamp current evoked by brief iontophoretic current pulses while the pipette was slowly retracted in steps of 0.5 μm. When the pipette tip was close to the varicosity, a brief current pulse (-100 nA, 0.5 ms) evoked a transient inward current with peak amplitude of ~15 pA (Fig. 7b, top). As we

retracted the pipette along its long axis (X), we measured the peak inward current of the response evoked at each position (stimulus interval ≥ 20 s). When the pipette tip was further from the varicosity, the peak amplitude of the response declined and the rise time of the response increased (Fig. 7b, bottom), consistent with a longer time required for diffusion of glutamate from the tip of the pipette to the location of the receptors. The data points for the peak response amplitude versus pipette position were well fitted by a Gaussian function (Fig. 7c), with best-fit values for width (SD × √2) and peak of 5.1 μm and 17 pA, respectively. From the Gaussian function, we also estimated the full width at half-maximum as 8.5 μm (Fig. 7c). From these measurements, we can conclude that fast microiontophoresis can apply drug with a high degree of spatial precision and confinement.

2.18 Control Experiments for Microiontophoresis

It is important to control for indirect effects evoked by applying current through a microiontophoresis pipette, i.e., to understand if an observed response (electrophysiological and/or intracellular Ca^{2+}) is due to iontophoretic ejection of the neuroactive substance or to direct electrical stimulation. Several control experments can be performed, as suggested below.

1. When first setting up this technique in the laboratory, it can be useful to perform experiments where the microiontophoresis pipette contains only salt solution without active drug. Applying iontophoretic current of both positive and negative polarity can be used to test for direct effects of the electrical stimulation.

2. Reversing the polarity of the iontophoretic current can also be useful to verify a direct effect when applying a neuroactive substance. For example, if application of glutamate with negative current evokes a response, the stimulus can then be inverted (i.e., to a positive current) while keeping the other parameters (amplitude, duration) constant. If the response is still observed, it suggests that it is not due to iontophoretic ejection of glutamate.

3. If a response (electrophysiological, intracellular Ca^{2+}) is due to iontophoretic ejection of a neuroactive substance, as opposed to being directly evoked by the electrical stimulation itself, it should be possible to block the response by applying pharmacological blockers. If the response is reduced (or disappears) in the presence of a blocker, it is a good idea to examine if recovery can be observed after washout of the blocker.

4. When experiments combine electrophysiological recording and Ca^{2+} imaging and the goal is to investigate which ion channels are involved in mediating an intracellular Ca^{2+} response, one will typically control the membrane potential by recording with the voltage-clamp technique, thereby avoiding indirect effects mediated by postsynaptic depolarization and activation of voltage-gated Ca^{2+} channels. When recording from branched neurons, however, it can be difficult to achieve a satisfactory level of voltage control (space clamp) and avoid a local escape from the voltage-clamp potential in the dendritic tree. If one suspects that activation of voltage-gated Ca^{2+} channels is responsible for, or significantly contributes to, an observed response, this can be examined by repeating the test after hyperpolarizing the neuron relative to the original holding potential. Even with imperfect space clamp control, hyperpolarization will decrease the likelihood of reaching the level of depolarization required for opening of voltage-gated Ca^{2+} channels and with sufficient hyperpolarization, a response mediated by voltage-gated Ca^{2+} channels will be reduced or blocked. In contrast, if a Ca^{2+} response is mediated by influx through ligand-gated channels, voltage clamping the cell at a more hyperpolarized potential should only increase the driving force for Ca^{2+} influx and no reduction of the response should be observed.

5. It is also possible that a response (electrophysiological or intracellular Ca^{2+}) can be evoked indirectly by action potentials generated in presynaptic axons by electrical stimulation from the iontophoresis pipette. Such responses should display an all-or-none behavior with a distinct threshold. By varying the stimulus intensity (amplitude and/or duration), it should be possible to reveal if this is the case or not.

3 Notes and Trouble Shooting

Here we provide a list of potential problems and pitfalls that can occur during experiments that combine MPE structural and functional imaging, microiontophoretic drug application, and electrophysiological recording, together with suggestions for trouble shooting.

1. Problem: Attempted targeting of a specific subcellular structure with the microiontophoretic pipette is unsuccessful.
Possible reason: The pipette touches the tissue when it is moved downwards after retraction (position 3 in Fig. 4b).
Solution: For accurate targeting of the microiontophoretic pipette, it is necessary to measure the angle of the headstage of the microiontophoresis amplifier relative to the horizontal plane. Some micromanipulators come with a scale where the angle can be read directly, but the resolution may not be adequate. A very useful alternative for accurate measurement is to use a smartphone with a "Clinometer" app. The magnitude of the angle and the vertical distance between the target structure and the tip of the pipette (when located above the target; position 1 in Fig. 4b) determine the distance that the pipette should be retracted (position 2 in Fig. 4b) such that it does not move into the preparation when moving down to position 3 (Fig. 4b).

2. Problem: No electrophysiological or Ca^{2+} response is observed during microiontophoretic drug application.
Possible reason: The tip of the microiontophoresis pipette is too far from the targeted structure.
Solution: Move pipette closer (under visual control, i.e., during MPE imaging).

Possible reason: The tip of the microiontophoresis pipette is clogged.
Solution: Check the resistance of the pipette (following adequate capacitance compensation) and see if it has changed relative to the start of the recording. It is

sometimes possible to reduce the resistance of a clogged pipette by repeated application of large amplitude current pulses, but make sure to move the pipette tip away from critical target structures if attempting this. Afterwards, check the capacitance compensation and measure the resistance again. If it is not possible to reduce the resistance sufficiently, the pipette must be replaced.

Possible reason: The neuron (or the targeted subcellular structure) does not express receptors that can be activated by the applied drug.
Solution: Attempt an alternative and less demanding experiment to verify that the type of neuron investigated expresses ligand-gated ion channels that are activated by the applied drug. Apply the drug by pressure ejection from a pipette with a larger opening such that the drug reaches a larger area of the dendritic tree or soma region of the cell.

3. Problem: During functional imaging of intracellular Ca^{2+}, no response can be evoked by microiontophoretic activation of Ca^{2+}-permeable receptors presumed to be expressed by the targeted neuron (e.g. NMDA receptors or Ca^{2+}-permeable AMPA receptors).
Possible reason: There are many potential explanations why the expected response is not observed, but it is important to first verify that *any* Ca^{2+} response can be observed.
Solution: A simple way to verify that the intracellular solutions, including the fluorescent Ca^{2+} indicator, and the microscope hardware/software imaging system are working as expected, is to apply depolarizing voltage steps and image from a neuron and subcellular compartment known to express voltage-gated Ca^{2+} channels.

4. Problem: Over the course of an experiment, there is excessive drift and spatial separation between the tip of the microelectrode and the target structure.
Possible reason: It is impossible to completely avoid mechanical drift, but one explanation is that the shape of the micropipette is suboptimal, e.g. the taper is too short. If such a pipette is used, it will push the tissue and this can often be followed by

subsequent drift of the tip beyond the target structure after the absolute position of the pipette has been fixed.

Solution: It is important to use micropipettes with sufficiently long and slender tips for the iontophoretic application such that the pipette does not push the tissue too much as it is inserted into the slice. If possible, change the parameters of the pipette puller. To reduce the likelihood of drift during an experiment, only use high-quality micromanipulators and avoid abrupt changes of temperature at or near the setup. Such changes can be related to transient cooling or heating systems. If possible, try to shield the setup from such influences.

4 Outlook and Future Perspectives

Drug application by fast microiontophoresis has been used to study synaptic integration by applying agonists at different locations in the dendritic tree of hippocampal pyramidal neurons, including studying the interaction between glutamatergic excitation and GABAergic inhibition [6, 15]. In our laboratory, we have used the technique to investigate changes of the Ca^{2+} permeability of AMPA-type glutamate receptors in retinal amacrine cells [16]. The main advantage compared to conventional microiontophoresis is the compensation of the pipette capacitance. This enables the use of very brief pulses that allow for high spatial and temporal resolution of the drug application. When microiontophoresis is performed with high-resistance pipettes with long, slender tips, the mechanical damage inflicted on the neural tissue does not seem to have any serious consequences compared to other techniques that use electrodes for recording and stimulation. Compared to pressure application from fine-tipped micropipettes, microiontophoretic application involves no mechanical movement and is therefore compatible with high-resolution Ca^{2+} imaging of subcellular compartments where movement artefacts must be avoided.

The cost of adding equipment for fast microiontophoresis to a setup already equipped for electrophysiological recording and MPE imaging is modest. Microiontophoresis

however, cannot compete with the flexibility offered by (more expensive) 1-photon (1P) and multiphoton (MP) microscopic uncaging of neuroactive substances. Of these, 1P uncaging using UV light has a higher uncaging efficacy, but suffers from higher risk of phototoxicity and lower axial resolution, because of the wavelengths used and because uncaging takes place in a larger volume (compared to MP uncaging). MP uncaging has a much improved axial resolution, but is considerably more expensive to establish as it requires the addition of a second pulsed IR-laser to the setup (see chapters by Stein et al. and Tran-Van-Minh et al., this volume).

Acknowledgments

This research was supported by The Research Council of Norway (NFR 182743, 189662, 214216 to EH; NFR 213776, 261914 to MLV).

References

1. Silver RA, MacAskill AF, Farrant M (2016) Neurotransmitter-gated ion channels in dendrites. In: Stuart G, Spruston N, Häusser M (eds) Dendrites, 3rd edn. Oxford University Press, New York, pp. 217-257
2. Kew JNC, Davies CH, editors (2010) Ion Channels. From Structure to Function. Oxford University Press, New York
3. Zheng J, Trudeau MC (2015) Handbook of Ion Channels. CRC Press, Boca Raton
4. Denk W, Strickler JH, Webb WW (1990) Two-photon laser scanning fluorescence microscopy. Science 248:73-76
5. Higley MJ, Sabatini BL (2012) Calcium signaling in dendritic spines. Cold Spring Harb Perspect Biol 4:a005686
6. Müller C, Beck H, Coulter D, Remy S (2012) Inhibitory control of linear and supralinear dendritic excitation in CA1 pyramidal neurons. Neuron 75:851-864
7. Bootman MD, Berridge MJ, Putney JW, Roderick HL, eds (2012) Calcium Signaling. Cold Spring Harbor Laboratory Press, Cold Spring Harbor
8. Nguyen Q-T, Clay GO, Nishimura N, Schaffer CB, Schroeder LF, Tsai PS, Kleinfeld D (2008) Pioneering applications of two-photon microscopy to mammalian neurophysiology. In: Masters BR, So PTC (eds) Handbook of Biomedical Nonlinear Optical Microscopy. Oxford University Press, New York, pp. 715-734
9. Yasuda R, Nimchinsky EA, Scheuss V, Pologruto TA, Oertner TG, Sabatini BL, Svoboda K (2004) Imaging calcium concentration dynamics in small neuronal compartments. Sci STKE 219:pl5
10. Grimes WN, Li W, Chávez AE, Diamond JS (2009) BK channels modulate pre- and postsynaptic signaling at reciprocal synapses in retina. Nat Neurosci 12:585-592

11. Stone TW (1985) Microiontophoresis and Pressure Ejection. IBRO Handbook Series: Methods in the Neurosciences. General ed.: Smith AD. Wiley, Chichester
12. Lalley PM (1999) Microiontophoresis and pressure ejection. In: Windhorst U, Johansson H (eds) Modern Techniques in Neuroscience Research. Springer-Verlag, Berlin, pp. 193-212
13. Liu G, Choi S, Tsien RW (1999) Variability of neurotransmitter concentration and nonsaturation of postsynaptic AMPA receptors at synapses in hippocampal cultures and slices. Neuron 22:395-409
14. Murnick JG, Dubé G, Krupa B, Liu G (2002) High-resolution iontophoresis for single-synapse stimulation. J Neurosci Meth 116:65-75
15. Müller C, Remy S (2013) Fast micro-iontophoresis of glutamate and GABA: a useful tool to investigate synaptic integration. J Vis Exp 77:e50701
16. Castilho Á, Ambrósio AF, Hartveit E, Veruki ML (2015) Disruption of a neural microcircuit in the rod pathway of the mammalian retina by diabetes mellitus. J Neurosci 35:3344-3355
17. Geiger JRP, Bischofberger J, Vida I, Fröbe U, Pfitzinger S, Weber HJ, Haverkampf K, Jonas P (2002) Patch-clamp recording in brain slices with improved slicer technology. Pflügers Arch 443:491-501
18. Bischofberger J, Engel D, Li L, Geiger JRP, Jonas P (2006) Patch-clamp recording from mossy fiber terminals in hippocampal slices. Nature Prot 1:2075-2081
19. Davie JT, Kole MHP, Letzkus JJ, Rancz EA, Spruston N, Stuart GJ, Häusser M (2006) Dendritic patch-clamp recording. Nature Prot 1:1235-1247
20. Tsai PS, Kleinfeld D (2009) In vivo two-photon laser scanning microscopy with concurrent plasma-mediated ablation: Principles and hardware realization. In: Frostig RD (ed) In Vivo Optical Imaging of Brain Function, 2nd edn. CRC Press, Boca Raton, pp. 59-115
21. Mainen ZF, Maletic-Savatic M, Shi SH, Hayashi Y, Malinow R, Svoboda K (1999) Two-photon imaging in living brain slices. Methods 18:231-239

22. Dodt H-U, Frick A, Kampe K, Zieglgänsberger W (1998) NMDA and AMPA receptors on neocortical neurons are differentially distributed. Eur J Neurosci 10:3351-3357

23. Bers DM, Patton CW, Nuccitelli R (2010) A practical guide to the preparation of Ca^{2+} buffers. In: Whitaker M (ed) Calcium in Living Cells. Methods in Cell Biology, Vol. 99. Wilson L, Matsudaira P (series eds). Academic Press, Burlington, pp. 1-26

24. Euler T, Hausselt SE, Margolis DJ, Breuninger T, Castell X, Detwiler PB, Denk W (2009) Eyecup scope -- optical recordings of light stimulus-evoked fluorescence signals in the retina. Pflügers Arch 457:1393-1414

25. Pologruto TA, Sabatini BL, Svoboda K (2003) ScanImage: Flexible software for operating laser scanning microscopes. Biomed Eng Online 2:13

26. Langer D, van 't Hoff M, Keller AJ, Nagaraja C, Pfäffli OA, Göldi M, Kasper H, Helmchen F (2013) HelioScan: a software framework for controlling in vivo microscopy setups with high hardware flexibility, functional diversity and extendibility. J Neurosci Meth 215:38-52

27. Nguyen Q-T, Driscoll J, Dolnick EM, Kleinfeld D (2009) MPScope 2.0: A computer system for two-photon laser scanning microscopy with concurrent plasma-mediated ablation and electrophysiology. In: Frostig RD (ed) In Vivo Optical Imaging of Brain Function, 2nd edn. CRC Press, Boca Raton, pp. 117-142

28. Brown KT, Flaming DG (1986) Advanced Micropipette Techniques for Cell Physiology. IBRO Handbook Series: Methods in the Neurosciences. General ed.: Smith AD. Wiley, Chichester

29. Dutta-Moscato J (2007) Microiontophoresis as a Technique to Investigate Spike Timing Dependent Plasticity. MSc thesis, University of Pittsburgh

30. Nelson R, Kolb H (1985) A17: A broad-field amacrine cell in the rod system of the cat retina. J Neurophysiol 54:592-614

Figure Captions

Fig. 1 Electrophysiological recording from and imaging of *in vitro* retinal slices. (**a**) Schematic figure of recording chamber (with central area corresponding to bottom covered with glass coverslip) with vertical retinal slices held in place by grid made by U-shaped profile (platinum-iridium wire) and nylon wires. (**b**) Infrared videomicrograph of a vertical retinal slice at low magnification. The layering of the retina can be clearly visualized, with the ganglion cell layer at bottom and the photoreceptor outer segments at top. (**c**) Infrared videomicrograph of a patch pipette for whole-cell electrophysiological recording (left) and a high-resistance pipette for microiontophoretic application (right). Note the relatively large opening of the patch pipette and that the opening of the high-resistance pipette cannot be resolved by the light microscope. Bars, 50 μm (**b**), 10 μm (**c**)

Fig. 2 Tuning and compensation of the capacitance of a high-resistance pipette for microiontophoresis. The tuning was performed after filling the pipette with electrolyte and immersion into the recording chamber (as in Fig. 1) by applying current pulses of ±10 nA (5 ms duration). The capacitance setting of the microiontophoresis amplifier was adjusted to illustrate an undercompensated pipette (left), a correctly compensated pipette (middle), and an over-compensated pipette (right). The resistance of the pipette was approximately 95 MΩ

Fig. 3 Identification of neurons in vertical retinal slices for electrophysiological recording and multiphoton excitation (MPE) imaging. (**a-c**) Infrared videomicrographs of retinal slices with identified cell bodies (marked by asterisks) of an AII amacrine cell (**a**), bipolar cells (**b**), and an A17 amacrine cell (**c**). After establishing a whole-cell recording, fluorescent dye diffuses from the patch pipette into the cell (Alexa 594: **d**, **f**, and **g**; Lucifer yellow: **e**) and enables MPE microscopy to visualize the complete cellular morphology, as illustrated with maximum intensity projections for an AII amacrine cell (**d**), a rod bipolar cell (**e**), a cone bipolar cell (**f**), and an A17 amacrine cell

(**g**). Bars, 10 μm (**a**-**c**), 10 μm (**d**), 10 μm (**e**), 10 μm (**f**), 20 μm (**g**). Panel in (**g**) reproduced from Castilho et al. (2015) [16]

Fig. 4 Visually guided targeting of subcellular neuronal compartments of dye-filled neurons in *in vitro* slices using dye-filled microiontophoresis pipettes during MPE microscopic imaging. Schematic diagrams (**a**, **b**) show important stages of step-wise procedure. In this example, the neuron to be targeted has been filled with fluorescent dye via diffusion from a patch pipette during whole-cell recording. (**a**) First, with the help of MPE microscopy, the tip of the microiontophoresis pipette (at focal plane Z_2; upper broken horizontal line) is aligned (X, Y) with the center of the subcellular compartment (at focal plane Z_1; lower broken horizontal line) inside the slice preparation imaged along the vertical Z axis (broken vertical line). In both (**a**) and (**b**), the slice is seen from the side (along the Y axis). (**b**) Step-wise procedure for targeting the subcellular structure located a distance *b* below the surface of the tissue. In position 1, the tip of the pipette is aligned vertically above the target and is located a distance *a* above the surface of the tissue. The angle α between the pipette's long axis and the horizontal plane is 20°. In position 2, the pipette has been moved outward along its long axis by a distance *c* (indicated by the red color). In position 3, the pipette has been moved downwards (along the Z axis) a distance equal to *a*+*b*. In position 4, the pipette has been moved inwards again along its long axis corresponding (almost) to the distance *c*. (**c**) Screen shot from the ScanImage imaging software [25] corresponding to position 4 in (**b**) with MPE microscopy of the subcellular target (left; a dendritic varicosity of an A17 amacrine cell) and the distal part of the microiontophoresis pipette (right). For better display of fluorescent structures, the MPE image has been over-saturated. Here and later, the vertical line across the varicosity indicates the spatial extent of the line scan for Ca^{2+} imaging. (**d**) As in (**c**), but an example of suboptimal targeting of a subcellular structure (A17 dendritic varicosity) with a microiontophoresis pipette. The frame around the varicosity indicates the spatial extent of the frame scan for Ca^{2+} imaging

Fig. 5 Current and Ca^{2+} response evoked by subcellular microiontophoretic application of glutamate during whole-cell voltage-clamp recording and MPE microscopy of a neuron in a rat retinal slice. (**a**) Screen shot from ScanImage [25] with MPE microscopy of the subcellular target (left), a dendritic varicosity of an A17 amacrine cell (filled with 40 μM Alexa 594 and 200 μM of the Ca^{2+} indicator dye Oregon Green 488 BAPTA-1 [OGB-1] via the patch pipette), and the distal part of the microiontophoresis pipette (right; filled with 150 mM glutamate and 50 μM Alexa 594). (**b**) Inward current (recorded at a holding potential of -60 mV) evoked by microiontophoretic application of glutamate (-500 nA, 1 ms; 150 mM in pipette). Here, and in (**c**), the time of the iontophoretic current pulse is marked by the arrow above the trace. (**c**) Ca^{2+} signal from varicosity in (**a**) recorded simultaneously with current in (**b**). Ca^{2+} signal measured as relative change in fluorescence ($\Delta F/F$) of OGB-1

Fig. 6 Dose-response relationships for glutamate-evoked current and Ca^{2+} responses in a dendritic varicosity of an A17 amacrine cell during whole-cell voltage-clamp recording (holding potential -70 mV) and MPE microscopy (as in Fig. 5). Each response was evoked by microiontophoretic application of glutamate (150 mM in pipette, 1 ms pulse duration) with increasing iontophoretic current pulse amplitude (from 0 to -500 nA, steps of -100 nA). (**a**) Current (magenta) and Ca^{2+} (green) responses evoked by iontophoretic pulses of glutamate (arrows). (**c**) Peak amplitude of Ca^{2+} responses ($\Delta F/F$; green circles), peak amplitude of current responses (I_{peak}; magenta squares), and integral of current responses ($Q_{response}$; black triangles) as a function of iontophoretic stimulus charge (Q_{ionto}; product of iontophoretic current pulse amplitude and duration). Note increasing responses with increasing stimulus strength. Ca^{2+} signal measured as relative change in fluorescence ($\Delta F/F$) of OGB-1

Fig. 7 Estimating the spatial profile of glutamate applied by brief current pulses from a high-resistance microiontophoresis pipette in a rat retinal slice. (**a**) Screen shot from ScanImage [25] with MPE microscopy of the subcellular target (left), a dendritic varicosity of an A17 amacrine cell (filled with 40 μM Alexa 594 and 200 μM of the Ca^{2+} indicator dye OGB-1 via the patch pipette), and the distal part of the microiontophoresis pipette (right; filled with 150 mM glutamate and 50 μM Alexa 594). Voltage-clamp recording with a holding potential of -80 mV. (**b**) Current responses evoked by brief iontophoretic pulses of glutamate (-100 nA, 0.5 ms) with the pipette tip close to the dendritic varicosity (top; single average of responses obtained with the pipette tip 0, 0.5, 1, and 1.5 μm from the reference position) or further away from the dendritic varicosity (bottom; single average of responses obtained with the pipette tip 4, 4.5, 5, and 5.5 μm from the reference position). The time of glutamate application indicated by the stimulus artefacts. (**c**) Peak response amplitude as a function of distance between the pipette tip and the reference position ("0 μm") during step-wise retraction of the pipette from the target structure. The reference position corresponds to the first position tested, with the minimum distance between the pipette tip and the target. The response at each position is the average of three repetitions. The data points have been fitted with a Gaussian function, $I(x) = I_{peak} \times exp\left[-\left(\frac{x-x_0}{w}\right)^2\right]$, where I_{peak} is the peak amplitude, x_0 is the value at the center, and w is the width

Table Captions

Instrument parameters for pulling high-resistance (90 to 120 MΩ) microionto-phoresis pipettes suitable for *in vitro* tissue slices using the Flaming Brown P-97 pipette puller (Sutter Instrument). The parameters were tuned for a heating filament of the "trough" type and the "pressure" parameter was set to 200. Each line corresponds to one step of a two-step pull

Table 1.

Heat	**Pull**	**Velocity**	**Time**
325	0	30	200 - 250
325	55	85 - 90	200 - 250

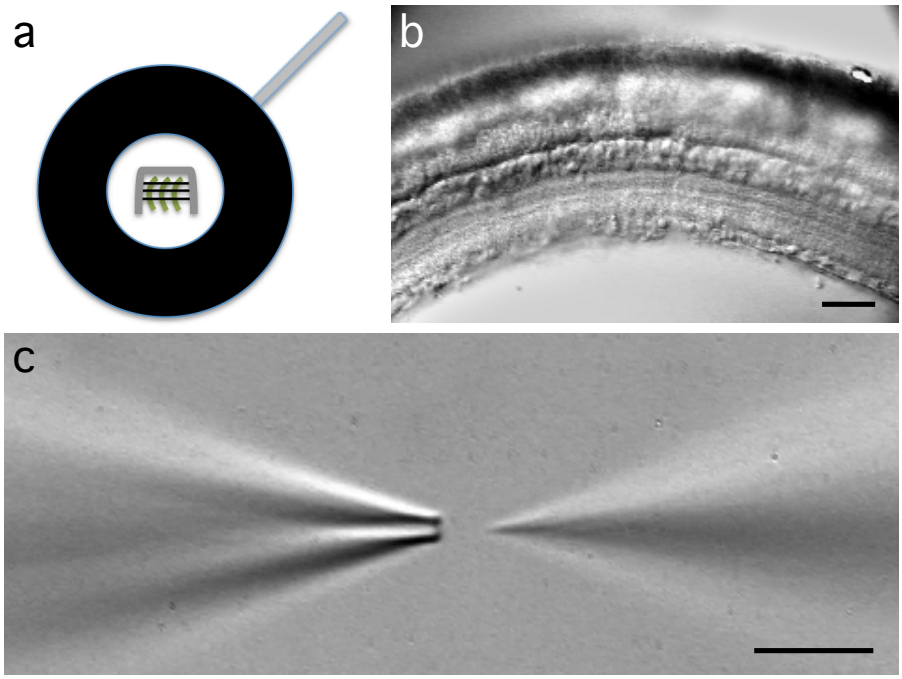

Figure 1 (Hartveit & Veruki)

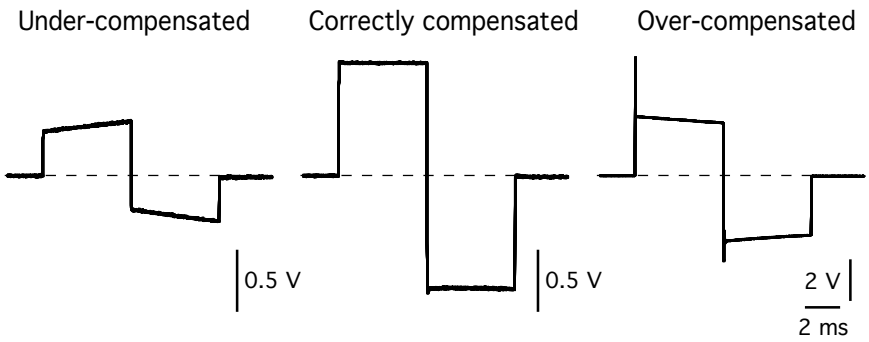

Figure 2 (Hartveit & Veruki)

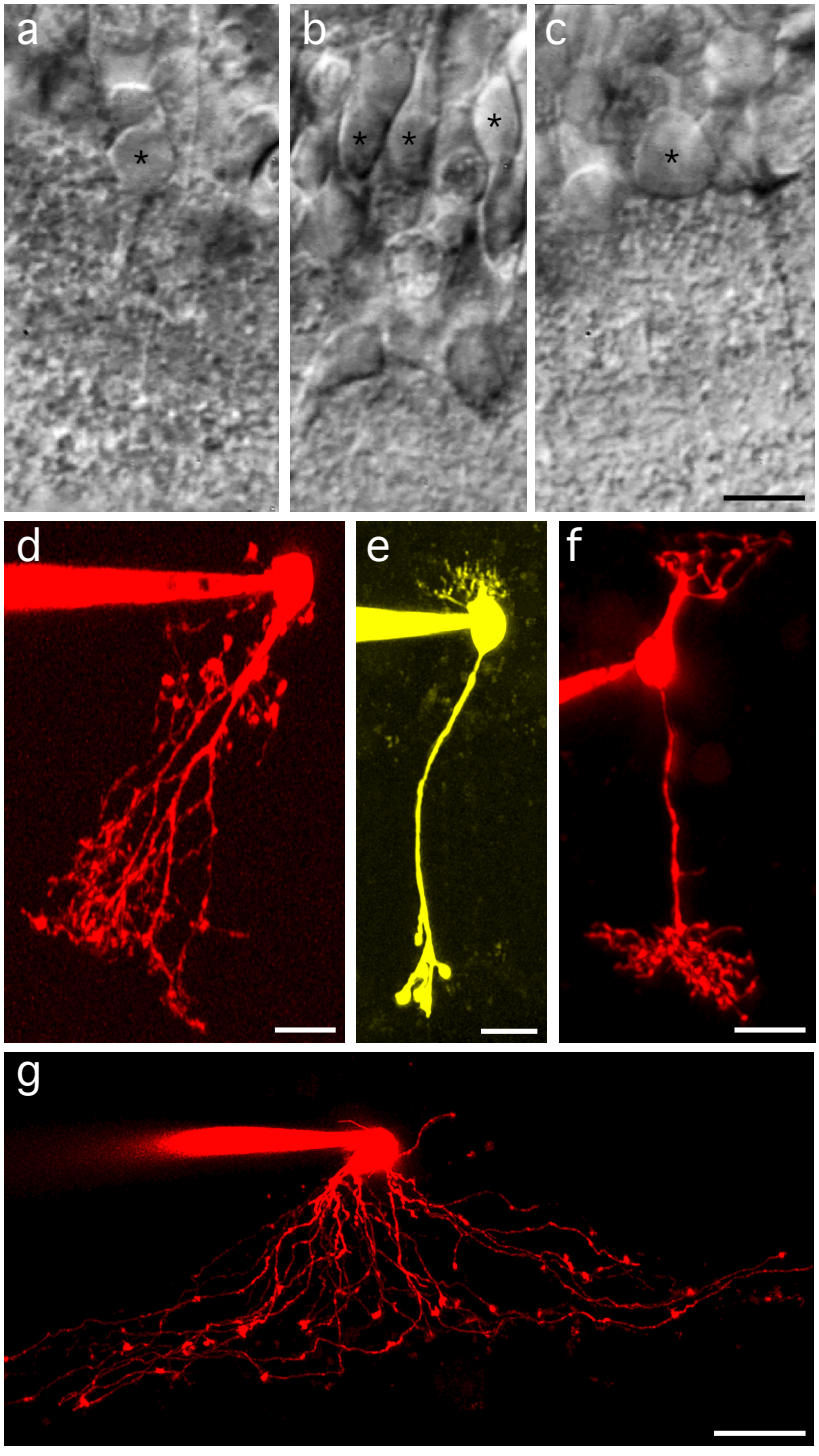

Figure 3 (Hartveit & Veruki)

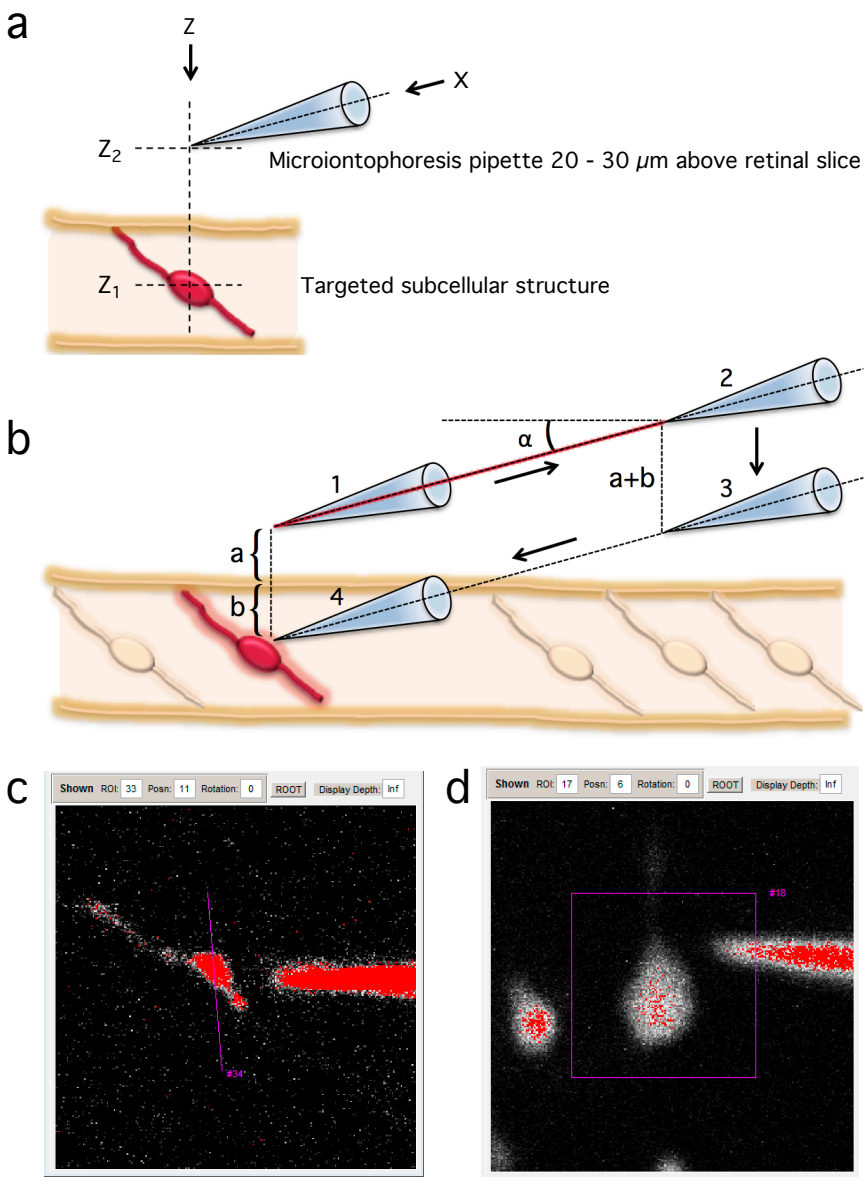

Figure 4 (Hartveit & Veruki)

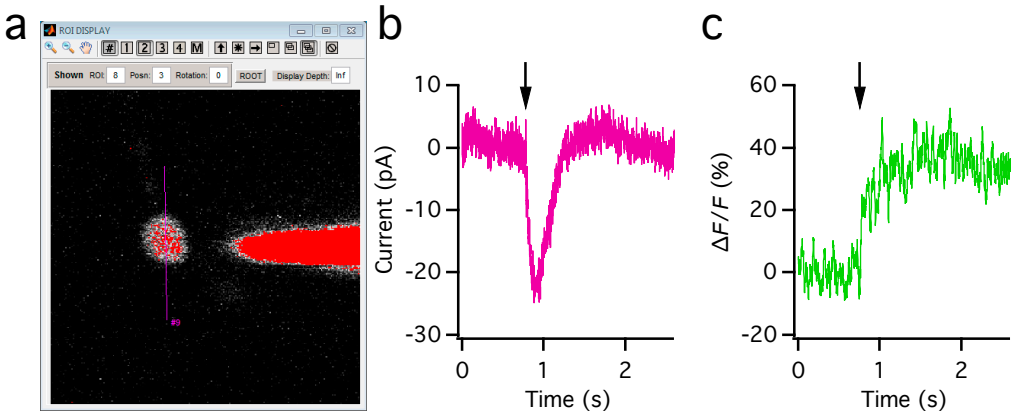

Figure 5 (Hartveit & Veruki)

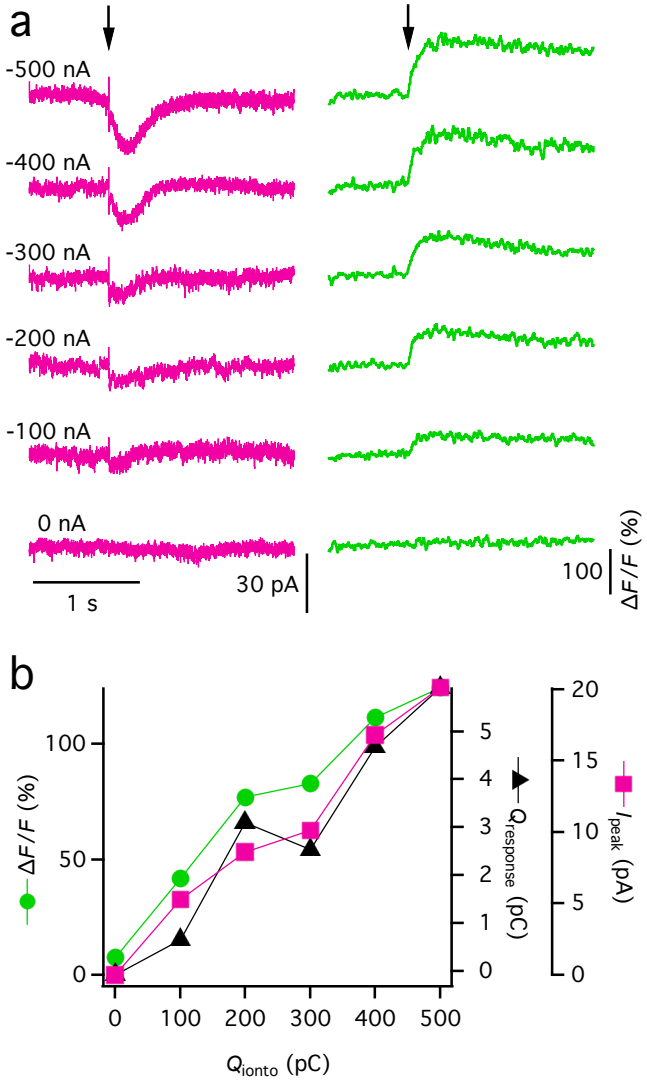

Figure 6 (Hartveit & Veruki)

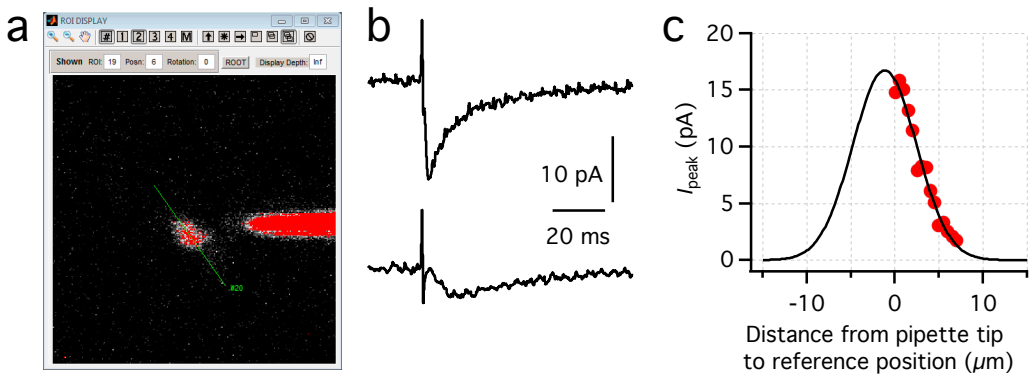

Figure 7 (Hartveit & Veruki)